ISSN 1330-3651 (Print), ISSN 1848-6339 (Online) https://doi.org/10.17559/TV-20211025173605
Original scientific paper

Experimental and Numerical Studies on Improvement of Aerodynamic Performance of a Semi-trailer Truck Model Using the Cabin Spoiler

Stjepan GALAMBOŠ, Nenad POZNANOVIĆ*, Nebojša NIKOLIĆ, Dragan RUŽIĆ, Jovan DORIĆ

Abstract: The paper presents the procedure of design, analysis and verification of the geometric parameters of the airfoil-shaped aerodynamic spoiler on the cabin of a semi-trailer truck. The procedure was carried out in order to obtain the optimal geometric shape and position of the spoiler, which will reduce the aerodynamic drag of a semi-trailer truck. The procedure for optimizing the geometric shape and position is based on Design of Experiments and Response Surface Methodology. The research included virtual experiments, realized by Computational Fluid Dynamics simulation, and physical experiments in a wind tunnel. A small-scaled model of a semi-trailer truck was used for the optimization of the shape and position of the aerodynamic spoiler. The achieved results were confirmed by experimental tests in a wind tunnel.

Keywords: aerodynamic drag force; aerodynamic spoiler; airfoil; CFD; DoE; semi-trailer truck; wind tunnel test

1 INTRODUCTION

The aerodynamics of motor vehicles is an important scientific discipline that has a great impact on many aspects regarding the proper behaviour of vehicles during operation. Large overall dimensions and most often unfavourable aerodynamic shapes make a semi-trailer truck a suitable test object. A large number of kilometres travelled during the truck exploitation, increases the need for improvement in the field of external aerodynamics. By reducing the aerodynamic drag on certain parts of the semi-trailer truck, as well as by properly redirecting the air flow, the overall aerodynamic drag of the semi-trailer truck will be reduced, which directly reflects on a lower fuel consumption.

Mohamed and Filippone in their work [1] point out the importance of aerodynamics in commercial vehicles intended for long-distance transport. The authors, in their work, present a numerical model for calculating the fuel consumption of commercial vehicles and conclude that the correct adoption of aerodynamic shapes achieves savings in fuel consumption of 9% per year with 130000 kilometres travelled. The simple existing solutions of aerodynamic accessories of commercial vehicles and analysis of their significance are presented by Wood and Bauer in their work [2]. They achieved fuel savings of 10% at three different velocity modes.

Unfavourable geometric shapes of commercial vehicles and large air gaps between the elements of the body contribute to the creation of local aerodynamic drag in the form of vortex air flow. This phenomenon, as well as the definition of the areas in which the greatest local drag occurs, is presented by Wood in [3] and Tyrrell in [4].

Computational Fluid Dynamics (CFD) is a powerful tool for describing real phenomena in the field of vehicle aerodynamics through simulations. This tool significantly contributes to saving time creating a virtual experiment and performing a large number of repetitions. Numerical CFD analysis of air flow propagation around a semi-trailer truck model is presented by Nakamura et al. in [5]. They conducted their research using LES (Large Eddy Simulation), which is important in studying the external aerodynamics of vehicles. The paper analyzes the influence of crosswind on the examined model. Analysis of air flow propagation by CFD simulations in the area between the vehicle floor and the road is presented in detail in [6] by Huminic A. and Huminic G. Simulation of thre E-dimensional air flow was performed using a RANS (Reynolds Average Navier-Stokes) model for a larger spectrum of velocities and the values of Reynolds number between 2.3×10^6 and 13.8×10^6.

A turbulence model has a great influence on the simulation results. Buljac et al. in [7] studied influence of the race car underbody, front and rear wings on aerodynamic forces using computational simulations and field experiments. The simulations are performed assuming the steady viscous flow and using the Reynolds-averaged Navier-Stokes equations along with the standard SST (Shear Stress Transport) k-omega turbulence model. In general, the rear diffuser at the trailing edge of the car underbody, the front and rear wings have proved to benefit the race car aerodynamics. Wilcox in [8] emphasizes the advantages and significance of the k-omega turbulence model. A three-dimensional k-epsilon turbulence model is applied by Galamboš et al. in [9]. Using the example of the air flow through the intake manifold of the internal combustion engine, the authors clearly define the advantages of using this type of turbulent flow in combination with a model prismatic polyhedral volumetric mesh.

There are a large number of mathematical methods and procedures that are used to reach an optimum in the analysis of the problem to be solved. A commonly used optimization procedure, which leads to a good setting of the experiment, is the Design of Experiment (DoE). The procedure was used by McCallen et al. in [10], where they presented the analysis of existing as well as the creation of improved aerodynamic spoilers. The paper combines the use of CFD simulations and experimental measurements in a wind tunnel.

It is well known that airfoils create aerodynamic drag force and lift force, but they also can be used in the exterior aerodynamics of motor vehicles to achieve a more favourable shape of the air flow around individual elements on the body. The analysis of the air flow around the airfoil marked SM701 with emphasis on the most important geometric parameters for design, is presented by Steen et al. in [11]. The analysis was performed for Reynolds

number values between 7×10^5 and 1.6×10^6. Numerical research of medium-heavy trucks, for the purpose of reducing the force of aerodynamic drag, is presented by Norouzi et al. in [12]. The flow field and pressure distribution around the truck were simulated using the Finite Volume Method. For the turbulent regime, the standard k-epsilon model was used to simulate the turbulent flow characteristics. The effects of vortices around the vehicle on the drag coefficient were studied. Bonitz et al. in [13] point to the negative impact of vehicle body accessories on the creation of local resistance. The test was performed on a Volvo S60 with a CFD simulation created using the k-epsilon turbulent model and a mesh model with a base cell size between 3 and 7 mm.

Reviewing the relevant literature covering the optimization of aerodynamic accessories of commercial vehicles, the authors of this paper found no reference dealing with the optimization of the airfoil shape and position for the purpose of its application in an aerodynamic accessory on a semi-trailer truck cabin. This motivated the authors to do a research in that direction. To that end, an optimization procedure has been devised, combining a few known methods.

First of all, a scaled CFD model of a semi-trailer truck without a spoiler has been created and verified experimentally in the wind tunnel. Then, the verified model has been used in the optimization procedure of airfoil parameters. The first step of the optimization procedure was to define airfoil parameters and to conduct a coarse analysis of their influence on the aerodynamic drag force of the semitrailer truck. The analysis was performed for all the parameter level combinations by using Full Factorial DoE with the aim to identify the area of optimal solution. In that area a more detailed analysis was carried out. The analysis implied adapting the parameter boundaries, as well as increasing the number of parameter levels. This was done by the Response Surface Methodology (RSM) based on Central Composite Design. By applying regression analysis on the RSM results, the response surface equation was formed. Finally, by minimizing the response surface equation the optimal shape and position of the airfoil were determined.

2 SIMULATION MODEL

The object of the research is a vehicle of typical semi-trailer truck configuration and geometry. For this purpose, a 3D CAD model of truck and semi-trailer, scaled 1:10, was created, with simplifications that do not have a direct impact on aerodynamic performance.

Using CAD model, a physical model of the semi-trailer truck was made (shown in the section "Experimental testing"). Fig. 1 shows the CAD model of a base configuration semi-trailer truck without a spoiler on the cabin.

The CAD model served as a basis for the development of the same-sized CFD model. The software that was used for CFD simulations is the CD Adapco-Star CCM+. After importing the CAD model into the CFD software, the necessary adjustments were made. In order to simulate the behaviour of a scaled physical model in a wind tunnel, an additional 3D CAD model of the wind tunnel was created, based on the model of the actual experimental set-up described in the section "Experimental testing". The front area of the semi-trailer truck model is $A = 0.0979$ m^2. The wind tunnel model, which is the domain of the simulation, is of semi-cylinder shape. The length of the tunnel model is 5000 mm and the radius is 600 mm. The CAD model of the semi-trailer truck is 5 mm away from the tunnel floor, in order to reduce the effect of the boundary layer.

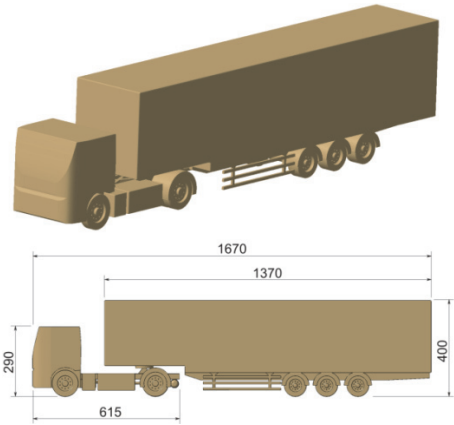

Figure 1 CAD model of a 1:10 scaled semi-trailer truck (dimensions are in millimetres)

The boundary conditions of the Velocity Inlet and Pressure Outlet, were set for the entrance and exit of the tunnel, respectively, while the Wall boundary condition was chosen for all solid surfaces of the model (semi-trailer truck model and tunnel model).

The range of air flow velocities has been chosen between 60 to 90 km/h. The calculated values of the Reynolds number for the scaled model length of 1.67 m are between 1.8×10^6 and 2.7×10^6, which clearly indicates turbulent flow.

Turbulence model is chosen to be Reynolds Averaged Navier Stokes (RANS) Realizable k-epsilon. The two-layer model that resolves the viscous sub-layer is combined with both the high and the low y+ wall treatment (so called all y+ wall treatment).

The flow was treated as a steady state and isothermal. The flow equations are solved in a segregated manner, one equation for velocity and one equation for pressure. The segregated flow solver uses the Semi-Implicit Method for Pressure Linked Equations (SIMPLE) algorithm. Simulation convergence criterion is based on normalized residuals. The root mean squared value of residuals of 10^{-3} has been chosen. Drag force and drag coefficient convergence and stability around converged value during the iteration served as additional criteria for judging the model setup.

The mesh settings of the CFD model involved adopting the mesh type and the size of the mesh base cell. Based on the recommendations from references [14-16], a prismatic polyhedral type of volumetric unstructured mesh was used because it is suitable for complex geometries and generally contains smaller number of cells than other types of mesh. The fluid region boundary surface is divided into the semi-trailer truck surface and the tunnel surface. The tunnel surface consists of entrance, exit, floor and tunnel wall, all with the same base cell surface size. The base cell size indicates edge lengths on the surface mesh. The mesh around the semi-trailer truck is much more refined in

comparison to the tunnel mesh. The target cell size and the minimum cell size at the semi-trailer truck surface are set to be 10% and 5% of the tunnel base cell, respectively. The ratio between the tunnel cell size and the semi-trailer truck cell size was kept constant in all simulations. Since only the gross flow features (total drag force and drag coefficient) are investigated, for the sake of computational efficiency, a coarser, high y+ wall-function type mesh is used. The base cell size of the wind tunnel model was determined after the mesh independence analysis, Fig. 2.

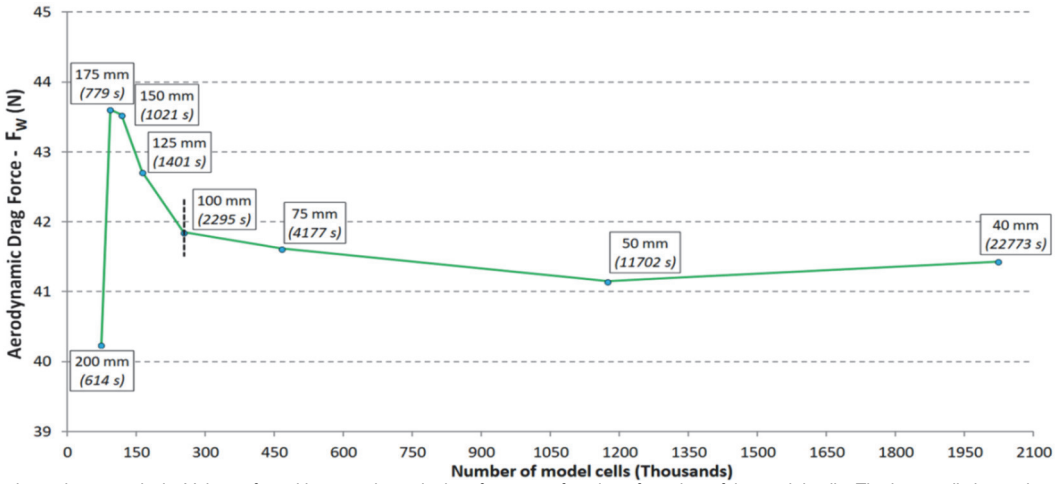

Figure 2 Mesh independence analysis. Values of resulting aerodynamic drag force as a function of number of the model cells. The base cell size and computational time are indicated at the graph

During the analysis, the number of cells has been varied by changing the base cell size of the tunnel. It was monitored how the number of cells affected the value of aerodynamic drag force F_w.

The analysis has been performed for the tunnel base cell size between 40 mm and 200 mm. For the cell size range between 40 mm and 100 mm, it turned out that the value of the aerodynamic drag force is changed less than 2%. However, computational time increases significantly with the mesh refinement. For the cell size of 40 mm computational time is about 10 times longer than for the cell size of 100 mm. In proposed spoiler profile optimization process, only the gross drag force post processed from CFD simulations is used as design response variable. In this research, it is considered that aerodynamic drag force resulting from the coarser model can be utilized as a decision variable for comparison of designs in the optimization process. The tunnel base cell size of 100 mm was chosen as a compromise between acceptable accuracy of the calculated drag force and computational efficiency. For that base cell size, the number of cells of the CFD model volumetric mesh is 252,686. Fig. 3 shows the CFD mesh model of the semi-trailer truck in the tunnel. After preliminary simulations, a stable CFD model has been used as an initial one for the spoiler optimization procedure.

On the initial model CFD simulations were performed for seven air flow velocity values from 60 to 90 km/h with an increment of 5 km/h. Tab. 1 shows obtained values of aerodynamic drag force and aerodynamic drag coefficient.

Table 1 Force and coefficient of aerodynamic drag of the initial semi-trailer truck CFD model

Air flow velocity v / km/h	Drag force F_W / N	Drag coefficient c_W / -
90	41.92	1.161
85	37.47	1.163
80	33.22	1.164
75	29.22	1.165
70	25.48	1.166
65	21.99	1.168
60	18.81	1.172

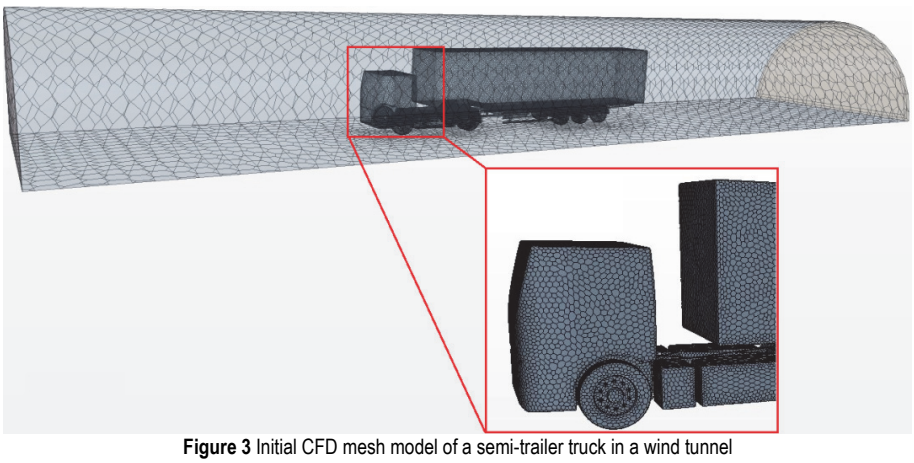

Figure 3 Initial CFD mesh model of a semi-trailer truck in a wind tunnel

3 THE OPTIMIZATION PROCEDURE OF THE AERODYNAMIC SPOILER

The aim is to find spoiler shape and position that minimize aerodynamic drag force of the semi-trailer truck. Spoiler position and airfoil-shaped cross-section are defined by four geometric parameters L, H, $R1$ and $R2$, Fig. 4.

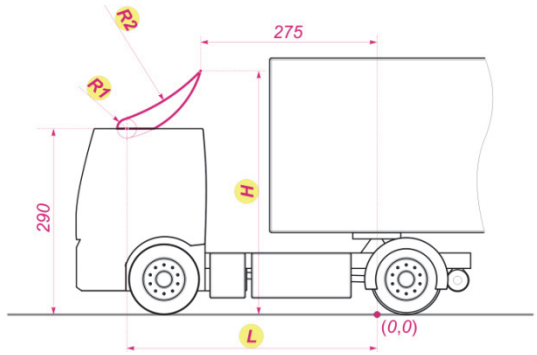

Figure 4 Geometric parameters of the cabin spoiler of the semi-trailer truck model (in mm)

3.1 Procedure Overview

As the optimization procedure the two-step sequential Design of Experiments was used. At the first step, thre E-level full factorial design is used to explore general system behaviour and main effects of the parameters on aerodynamic drag force. Based on results of this phase, the region of interest, the upper and lower limit for each of the parameters is adopted. In the second phase, a Response Surface Methodology based on Central Composite Design is used to estimate second order parameters interaction in the form of a quadratic response surface of aerodynamic drag force. Minimal value of response function is then used for determination of optimal value of parameters.

This procedure has been performed through a series of virtual experiments using the CFD simulation.

3.2 Full Factorial DoE

Three levels for each of the spoiler position and shape parameters were considered, Tab. 2.

Table 2 Full factorial DoE - parameter levels

Level code	H / m	L / m	$R1$ / m	$R2$ / m
−1	0.35	0.35	0.010	0.1
0	0.39	0.38	0.015	0.3
1	0.42	0.40	0.020	0.5

Four parameters with three different values yield a total of $3^4 = 81$ virtual experiments. All the experiments have been conducted at air flow velocity of 90 km/h. Fig. 5 presents graph with all 81 combinations of parameters and the values of aerodynamic drag force for each combination. Combination 16 (−1, 0, 1, −1) obtains minimum value of the aerodynamic drag force for full factorial design of experiment.

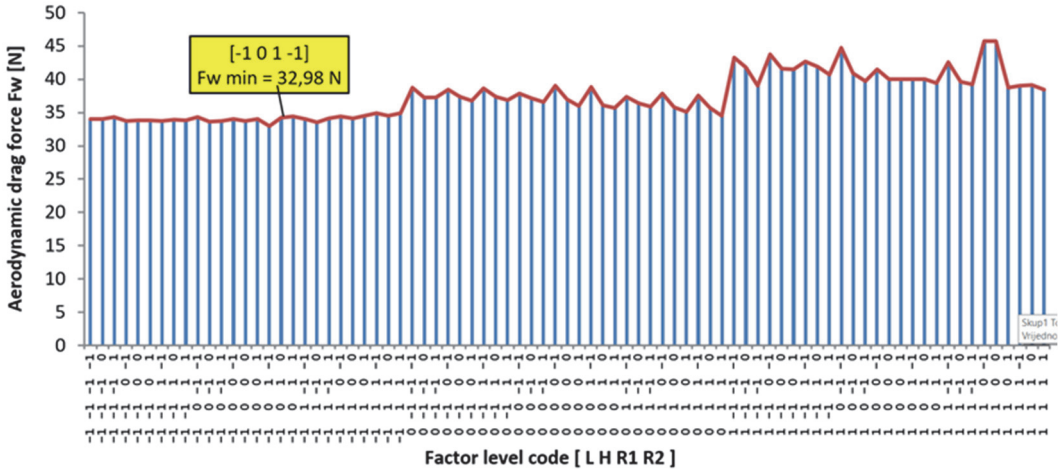

Figure 5 Results of Full Factorial Design of Experiment

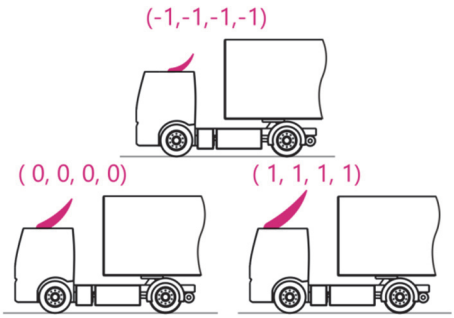

Figure 6 Configurations of the semi-trailer truck spoiler for the levels (−1, −1, −1, −1), (0, 0, 0, 0) and (1, 1, 1, 1) of the parameters L, H, $R1$ and $R2$

Examples of three typical configurations of the spoiler are shown in Fig. 6.

The results in Fig. 5 show that combination No. 16 provides the lowest aerodynamic drag force. The results of statistical analysis are shown in Fig. 7 in the form of Normal Probability Plot, Box Plot, Histogram and Main Effects Plot.

The P-value indicator with Normal Probability Plot (Fig. 7a) has a value less than 0.005, which indicates that the range of aerodynamic drag forces is statistically significant, because the P-value is less than 5%. Also, the value of Standard Deviation is 3.239%. The Box Plot (Fig. 7b) shows that the highest concentration of results is around the lower values, which is very important information, bearing in mind that the aerodynamic drag force should have the lowest possible value. The Histogram (Fig. 7c) shows the frequency of the results sequence from the smallest to the largest values. As in the

previous Fig. 7b, it can be concluded that the highest frequency of the results is around the lower values of the aerodynamic drag force, which increases the significance of the results sequence.

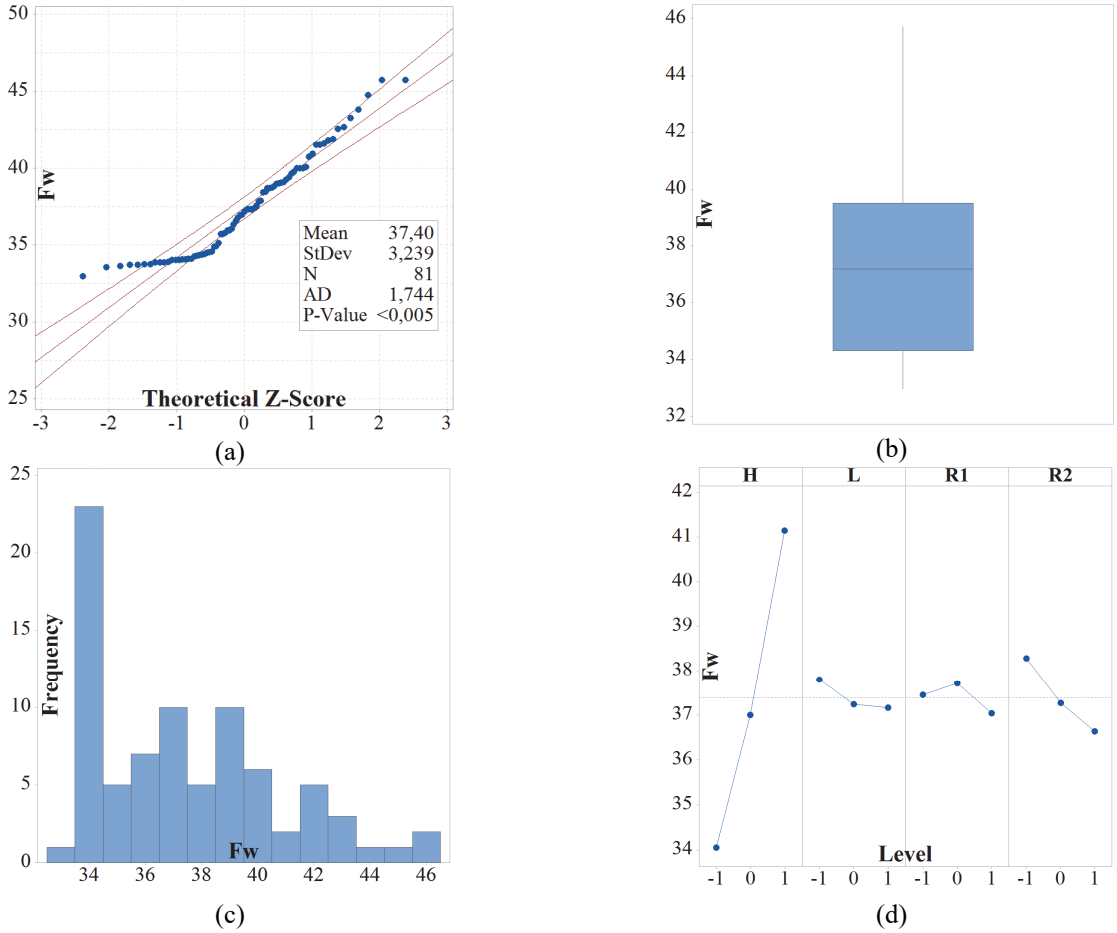

Figure 7 Aerodynamic drag force FW of the semi-trailer truck CFD model with the spoiler descriptive statistics of full factorial design of experiment (Fig. 5): (a) Normal probability plot, 95% CI; (b) Box plot; (c) Histogram; (d) Main Effects Plot

The Main Effects Plot (Fig. 7d) shows how each value of each parameter affects the result. Based on this presentation, it can be concluded in which direction the parameters should be varied, in order to obtain a better result. Also, if a parameter has very little effect on the result, it can be considered constant in the further optimization process. Fig. 7d shows a clear dominance of the influence of the parameter *H* on the aerodynamic drag force. The influence of the parameter *R*2 is significantly smaller, while the parameters *L* and *R*1 have the least influence on the aerodynamic drag force.

3.3 Response Surface Method

In this phase, the full factorial design is augmented by using the five-level Central Composite Design (CCD), [17-19]. Because of additional parameter levels, CCD allows estimation of response surface curvature. Tab. 3 shows the adopted parameter values.

Table 3 Parameter levels at Central Composite Design of experiment

Level code	*H* / m	*L* / m	*R*1 / m	*R*2 / m
−2	0.38	0.34	0.010	0.3
−1	0.39	0.35	0.015	0.4
0	0.40	0.36	0.020	0.5
1	0.41	0.37	0.025	0.6
2	0.42	0.38	0.030	0.7

The CCD yields 31 possible experimental settings, the last 7 of which are the same central points of the design and have same value. CFD simulations are performed according to the schedule in Tab. 5. The results are also presented in Tab. 4.

Main Effects analysis for five levels of parameters *H*, *L*, *R*1 and *R*2 at central composite design of experiment is shown in Fig. 8. Thanks to the main effect analysis shown in Fig. 8, the means at each level of a parameter can be analysed. This type of analysis can be used to compare the relative strength of the effects across parameters. Also, it can be proof for good choice of parameters values in the initial experiment setup (number and levels of parameters and value for each level code).

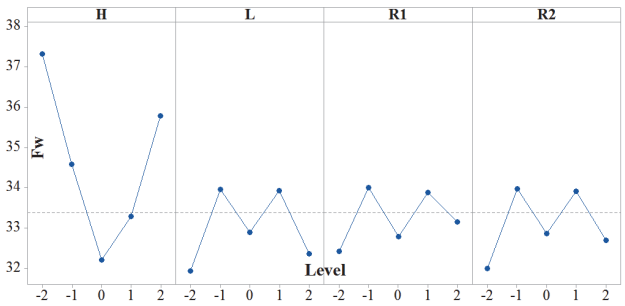

Figure 8 Main Effects Plot for five levels of parameters *H*, *L*, *R*1 and *R*2 at central composite design of experiment

Table 4 Results of Central Composite Design of experiment

Combination №	Factor level code				CFD simulation results	
	H	L	$R1$	$R2$	Drag coefficient c_w / -	Drag force F_w / N
1	−1	−1	−1	−1	0.945	34.11
2	−1	1	−1	−1	0.943	34.06
3	1	−1	−1	−1	0.948	34.23
4	1	1	−1	−1	0.936	33.79
5	−1	−1	1	−1	0.966	34.88
6	−1	1	1	−1	0.917	33.10
7	1	−1	1	−1	0.970	35.03
8	1	1	1	−1	0.901	32.55
9	−1	−1	−1	1	0.946	34.15
10	−1	1	−1	1	0.940	33.95
11	1	−1	−1	1	0.949	34.26
12	1	1	−1	1	0.926	33.45
13	−1	−1	1	1	0.962	34.74
14	−1	1	1	1	0.904	32.64
15	1	−1	1	1	0.977	35.26
16	1	1	1	1	0.908	32.79
17	0	−2	0	0	1.033	37.32
18	0	2	0	0	0.991	35.78
19	−2	0	0	0	0.884	31.93
20	2	0	0	0	0.896	32.36
21	0	0	−2	0	0.897	32.41
22	0	0	2	0	0.918	33.15
23	0	0	0	−2	0.886	31.99
24	0	0	0	2	0.905	32.69
25	0	0	0	0	0.887	32.03
26	0	0	0	0	0.887	32.03
27	0	0	0	0	0.887	32.03
28	0	0	0	0	0.887	32.03
29	0	0	0	0	0.887	32.03
30	0	0	0	0	0.887	32.03
31	0	0	0	0	0.887	32.03

The coefficients in the response surface function of aerodynamic drag force, Eq. (1), are obtained by regression analysis of the data from Tab. 4. The response surface coefficients are derived for uncoded parameter units.

$$\begin{aligned} F_{Wh} &= 44.53 - 5.910 \cdot H - 0.561 \cdot L - 0.422 \cdot R1 - \\ &-0.968 \cdot R2 + 1.2114 \cdot H^2 + 0.1106 \cdot L^2 + \\ &+0.2688 \cdot R1^2 + 0.1599 \cdot R2^2 - 0.1291 \cdot H \cdot L - \\ &-0.4578 \cdot H \cdot R1 - 0.0523 \cdot H \cdot R2 + \\ &+0.0513 \cdot L \cdot R1 + 0.0519 \cdot L \cdot R2 + 0.0159 \cdot R1 \cdot R2 \end{aligned} \quad (1)$$

Presented equation describes the model behaviour with an accuracy of 95.8%.

Table 5 Parameter values that provide the minimum aerodynamic drag

Parameter	Value / m
H	0.3627
L	0.4002
$R1$	0.0210
$R2$	0.4912

The parameter values that provide the minimum of the aerodynamic drag force response function are determined by numerical quasi-Newton minimization, Tab. 5.

By applying parameter values from the Tab. 6 to the CFD model, an aerodynamic drag force of 31.75 N was obtained. Fig. 9 shows the optimized spoiler design.

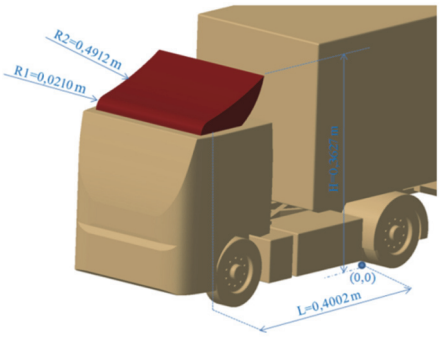

Figure 9 Aerodynamic spoiler on the truck cabin based on optimized parameter values

4 EXPERIMENTAL TESTING

The purpose of the experimental testing is to verify the CFD simulations and the results of the optimization process. The experimental testing was conducted in the "Miroslav Nenadović" wind tunnel within the Faculty of Mechanical Engineering in Belgrade, Serbia. It is a closed type of underground wind tunnel with a circular air flow. The main dimensions of the testing space are 6 × 2.9 × 2.1 meters. Maximum air velocity of 116 m/s is reached by a four-blade fan with the motor electrical power of 200 kW.

For the purpose of measuring aerodynamic drag force, which is a horizontal component of vehicle resistance, an aerodynamic drag force measuring facility was built. Fig. 10 shows a schematic representation of the facility for measuring the aerodynamic drag force of the semi-trailer truck model in a wind tunnel. This model, with dimensions of 1670 × 255 ×400 mm, is made of wood in a scale of 1:10 compared to the actual semi-trailer truck. The models of the truck 1 and the semi-trailer 2 are attached to the board 9 via a support. The models 1 and 2 are raised above the board at a vertical distance of 5 mm as it is in CFD model. The board 9 is fastened via sliders 5 to sliding guides 6 through which the longitudinal translational movement of the board 9 is provided, together with models 1 and 2. The board 9 rests at the force measuring cell 8. The measuring cell CZL623B -20kg was used with the comprehensive full scale error 0.03% and rated output 2 ± 0.02 mV/V. The signal from the measuring cell is transferred to the universal measuring amplifier HBM QuantumX MX840A. Data acquisition was performed by the software HBM catman Easy -AP ver. 3.5.1.

Experimental measurements were performed on the following configurations of the measuring facility:

- Aerodynamic drag force measurement of board 9 only, without the semi-trailer truck model.
- Aerodynamic drag force measurement of the semi-trailer truck model without an aerodynamic spoiler;
- Aerodynamic drag force measurement of the semi-trailer truck model with aerodynamic spoiler on the cabin of the truck.

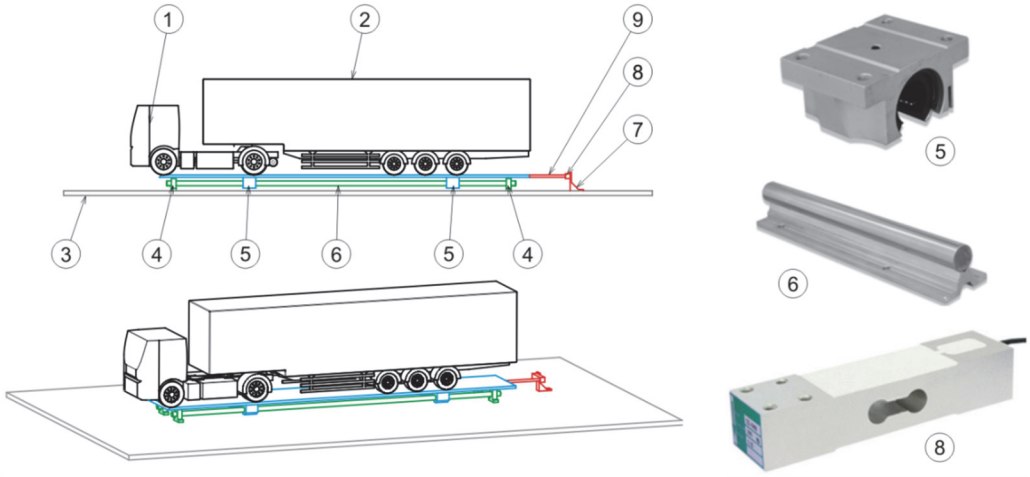

Figure 10 Aerodynamic drag force measuring facility in a wind tunnel

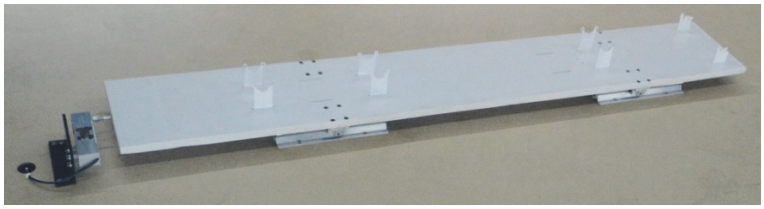

(a)

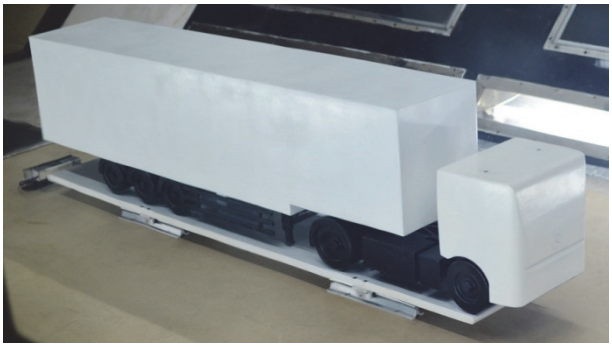

(b)

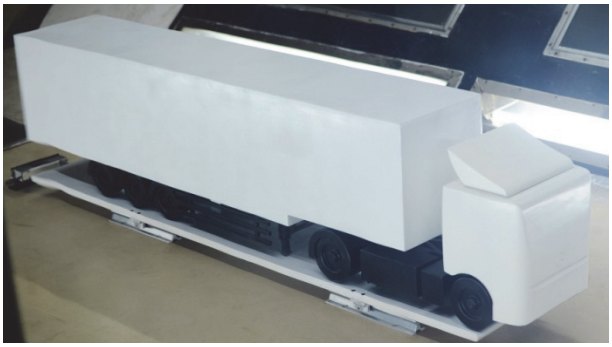

(c)

Figure 11 Test model in the wind tunnel. (a) Board without the model; (b) Model without aerodynamic spoiler; (c) Model with aerodynamic spoiler

Fig. 11 shows the actual model configurations during measurements in the wind tunnel.

Within each measuring facility configuration, one measurement involved reading the aerodynamic drag force value at a single air flow velocity mode. Measurements were performed at seven velocity values in the range of 60 to 90 km/h, with an increment of 5 km/h. At each velocity mode, two measurements were performed for about 20 seconds. Thus, for each configuration of the measuring facility, 14 measurement records were obtained, which is illustrated in Fig. 12 for the semi-trailer truck model with the aerodynamic spoiler. Mean value of aerodynamic drag force for each velocity mode is shown above the appropriate measurement record data.

5 RESULTS AND DISCUSSION

The results of one experimental measurement are presented as the average of the corresponding measurement record values. The results of the corresponding CFD simulations were compared with the experimental results, and their relative deviation was determined according to Eq. (2):

$$\Delta F_{W\,i} = \frac{\Delta F_{W\,\mathrm{CFD}} - F_{W\,\mathrm{EXP}\,i}}{F_{W\,\mathrm{EXP}\,i}} \tag{2}$$

where $F_{W\,\mathrm{CFD}}$ represents the value of the aerodynamic drag force obtained by CFD simulation, $F_{W\,\mathrm{EXP}\,i}$ is the averaged value of the measured aerodynamic drag force in one measurement record, and $i = \{1, 2\}$ is the ordinal number of measurements at one velocity mode.

Tab. 6 gives a comparative presentation of the results obtained by CFD simulations and experimentally for all three considered configurations and all velocity values from 60 to 90 km/h. $\Delta F_{W\,\mathrm{AVG}}$ is the arithmetic mean of the values $\Delta F_{W\,1}$ and $\Delta F_{W\,2}$.

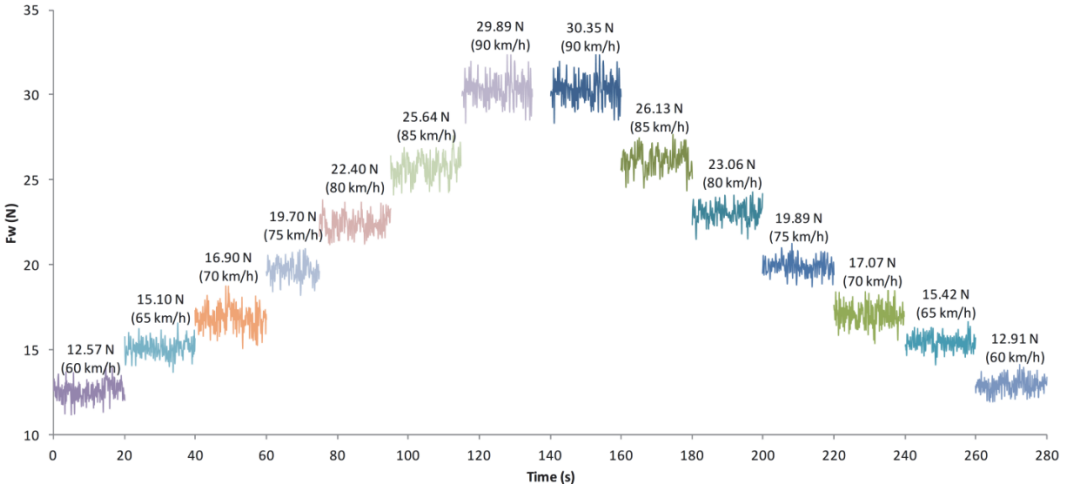

Figure 12 The measurement record of the semi-trailer truck model with aerodynamic spoiler on the truck cabin

Table 6 Comparative presentation of the obtained results

Configuration of the measuring facility	v / km/h	$F_{W\,CFD}$ / N	$c_{W\,CFD}$ / -	$F_{W\,EXP\,1}$ / N	$c_{W\,EXP\,1}$ / -	$F_{W\,EXP\,2}$ / N	$c_{W\,EXP\,2}$ / -	$\Delta F_{W\,1}$ / %	$\Delta F_{W\,2}$ / %	$\Delta F_{W\,AVG}$ / %
Board without the model	60	1.01	2.47	0.88	2.15	0.90	2.20	14.29	12.08	13.18
	65	1.18	2.45	1.04	2.16	1.04	2.16	13.40	13.68	13.54
	70	1.35	2.42	1.19	2.13	1.18	2.12	13.75	13.97	13.86
	75	1.55	2.42	1.36	2.12	1.37	2.14	14.24	13.14	13.69
	80	1.75	2.40	1.55	2.13	1.53	2.10	12.83	14.40	13.61
	85	1.97	2.40	1.53	1.86	1.77	2.15	11.25	12.43	11.84
	90	2.20	2.39	1.92	2.08	1.99	2.16	14.58	10.55	12.56
Model without aerodynamic spoiler	60	18.81	1.17	16.44	1.02	16.78	1.05	14.40	12.08	13.24
	65	21.99	1.17	20.01	1.06	20.23	1.07	9.90	8.69	9.29
	70	25.48	1.17	23.13	1.06	23.59	1.08	10.18	8.01	9.09
	75	29.22	1.17	26.87	1.07	27.09	1.08	8.75	7.86	8.30
	80	33.22	1.16	30.79	1.08	30.88	1.08	7.88	7.58	7.73
	85	37.47	1.16	34.95	1.08	35.17	1.09	7.21	6.52	6.86
	90	41.92	1.16	38.23	1.06	38.68	1.07	9.65	8.39	9.02
Model with aerodynamic spoiler	60	14.06	0.88	12.57	0.78	12.91	0.80	11.86	8.89	10.37
	65	16.48	0.87	15.10	0.80	15.42	0.82	9.17	6.85	8.01
	70	19.09	0.87	16.90	0.77	17.07	0.78	12.98	11.86	12.42
	75	21.88	0.87	19.70	0.79	19.89	0.79	11.08	9.99	10.53
	80	24.96	0.87	22.40	0.79	23.06	0.81	11.44	8.23	9.83
	85	28.13	0.87	25.64	0.80	26.13	0.81	9.70	7.66	8.68
	90	31.75	0.88	29.89	0.83	30.35	0.84	6.22	4.61	5.41

The obtained results in Tab. 6 show an acceptable agreement between the results achieved by CFD simulations and experimental tests in the wind tunnel. The deviation of $\Delta F_{W\,AVG}$ ranges between 4 and 15%. The adopted type of mesh and turbulent model within the CFD simulation provides good repeatability of the results for all considered airflow velocity values and all configurations of the measuring facility. Tab. 6 also shows aerodynamic drag coefficients c_W for all numerical and experimental combinations. Comparison was made for c_W calculated by simulations drag forces, between configurations with and without aerodynamic spoiler. That comparison shows average reduction of the aerodynamic drag coefficients of 33.2%. Also, same comparison was made for c_W calculated by experimental drag forces, between configurations with and without aerodynamic spoiler. Average reduction of the aerodynamic drag coefficients was 34%. Standard deviations for those comparisons were 3.4. Due to the correct rounding design of the board leading edge and its distance in relation to the tested model, a very small aerodynamic drag force of the board without the model was observed, with a value of order of 2 N at the highest considered air flow velocity.

In order to further confirm the adequacy of the developed CFD model, an additional comparison of the truck with and without the spoiler has been performed. Namely, aerodynamic drag force reduction on the truck with the spoiler, obtained by the simulation, has been compared to the corresponding experimental value under the same conditions. It was found that the reduction obtained by CFD simulation is very close to the reduction obtained experimentally, at all the velocities considered 24%.

Visualization of the air flow around the tested model configurations was performed via CFD simulations. Fig. 13 shows a comparative view of air velocity streamlines around the model configurations with and without the aerodynamic spoiler on the truck cabin. Fig. 13 shows a significant improvement in the air flow field in the area above and behind the truck cabin, as the vortex concentration is directly responsible for creating a local aerodynamic drag.

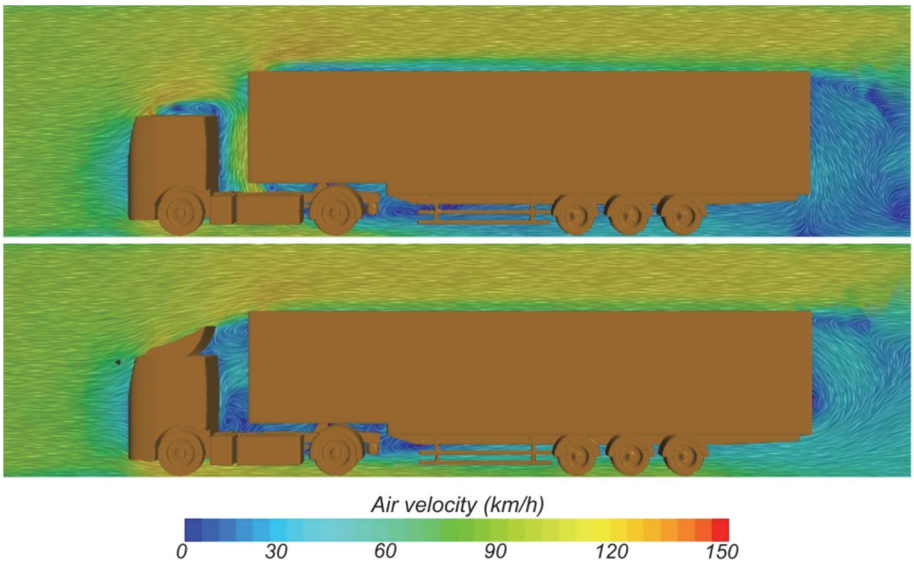

Figure 13 Comparative view of air flow fields around the model with and without the aerodynamic spoiler

6 CONCLUSIONS

The aim of the study was to develop a procedure of optimizing the airfoil shape and position for the purpose of its application in an aerodynamic accessory on a semi-trailer truck cabin. The research included virtual experiments, realized by CFD simulations and physical experiments in a wind tunnel. The simulations efficiency is achieved by a relatively coarse, but sufficiently representative CFD model. The procedure was conceived as a combination of several known methods: Full Factorial Design of Experiments, Central Composite design, regression analysis and minimization of Response Surface equation.

Four parameters defining the airfoil shape and position have been considered: top edge height from the ground (H), horizontal position of spoiler front radius centre (L), spoiler front edge radius ($R1$) and spoiler leading edge radius ($R2$). It turned out that parameter H has a dominant influence on the aerodynamic drag force. The influence of the parameter $R2$ is significantly smaller, while the parameters L and $R1$ have the least influence on the aerodynamic drag force.

As a result of Central Composite design of experiments, a quadratic response surface function of aerodynamic drag force was generated. Spoiler design parameters are optimized by minimizing the response surface function. CFD simulation results were validated by measurements in the wind tunnel.

The procedure presented in the paper obtained total drag force reduction is 25%, if the model without aerodynamic spoiler is compared to the model with optimized aerodynamic spoiler on the truck cab. This procedure also can be performed by introducing additional parameters, including parameters that describe variations in the third dimension of the spoiler. Although such a research requires much more virtual experiments to be performed, it could lead to further improvement of truck aerodynamics.

Acknowledgments

This research was funded by the Ministry of Education, Science and Technology Development of the Republic of Serbia as a part of the project 451-03-9/2021-14/200156: "Innovative scientific and artistic research from the FTS activity domain".

The authors would like to express their gratitude to the Laboratory of Aerotechnics at the Faculty of Mechanical Engineering, University of Belgrade for a very helpful cooperation during the experimental testing in their wind tunnel "Miroslav Nenadović".

7 REFERENCES

[1] Mohamed-Kassim, Z. & Filippone, A. (2010). Fuel savings on a heavy vehicle via aerodynamic drag reduction. *Transportation Research Part D: Transport and Environment*, *15*(5), 275-284. https://doi.org/10.1016/j.trd.2010.02.010

[2] Wood, R. M. & Bauer, S. X. S. (2003). Simple and Low-Cost Aerodynamic Drag Reduction Devices for Tractor-Trailer Trucks. *SAE Transactions*, *112*, 143-160. https://doi.org/10.4271/2003-01-3377

[3] Wood, R. M. (2006). A discussion of a heavy truck advanced aerodynamic trailer system. *Int. Symp. Heavy Veh. Weights Dimens., 9th, University Park, PA*, 1-14.

[4] Tyrrell, C. L. (1987). *Aerodynamics and Fuel Economy -On -Highway Experience* (SAE Technical Paper No. 872278). SAE International. https://doi.org/10.4271/872278

[5] Nakamura, S., Hively, E. M., & Conlisk, A. T. (2009). *LES Simulation of Aerodynamic Drag for Heavy Duty Trailer Trucks*. 1037-1043.

[6] Huminic, A. & Huminic, G. (2009). *CFD Study Concerning the Influence of the Underbody Components on Total Drag for a SUV*. https://doi.org/10.4271/2009-01-1157

[7] Buljac, A., Kozmar, H., & Džijan, I. (2016). Aerodynamic Performance of the Underbody and Wings of an Open - Wheel Race Car. *Transactions of FAMENA*, *40*(2), 19-34. https://doi.org/10.21278/TOF.40202

[8] Wilcox, D. C. (1998). *Turbulence modeling for CFD*, *2*. DCW industries La Canada, CA.

[9] Galamboš, S. L., Nikolić, N. M., Ružić, D. A., & Dorić, J. Ž. (2020). An approach to computational fluid dynamic air-flow simulation in the internal combustion engine intake manifold. *Thermal Science*, *24*(1 Part A), 127-136. https://doi.org/10.2298/TSCI180707063G

[10] Mc Callen, R., Salari, K., Ortega, J., Castellucci, P., Browand, F., Hammache, M., Hsu, T. Y., Ross, J., Satran, D., Heineck, J. T., Walker, S., Yaste, D., DeChant, L., Hassan, B., Roy, C., Leonard, A., Rubel, M., Chatelain, P.,

Englar, R., & Pointer, D. (2004). DOE's Effort to Reduce Truck Aerodynamic Drag-Joint Experiments and Computations Lead to Smart Design. *34th AIAA Fluid Dynamics Conference and Exhibit*, *1-0*. American Institute of Aeronautics and Astronautics. https://doi.org/10.2514/6.2004 -2249

[11] Steen, G., Nicks, O. W., & Heffner, M. (1992). *Further wind tunnel investigation of the SM701 airfoil with aileron and turbulators*. Texas A & M University.

[12] Norouzi, M., Pooladi, M. A., & Mahmoudi, M. (2016). Numerical investigation of drag reduction in a Class 5 medium duty truck. *Journal of Mechanical Engineering and Sciences*, *10*, 2387-2400. https://doi.org/10.15282/jmes.10.3.2016.15.0221

[13] Bonitz, S., Larsson, L., Lofdahl, L., & Broniewicz, A. (2015). Structures of Flow Separation on a Passenger Car. *SAE Int. J. Passeng. Cars-Mech. Syst.*, *8*(1), 177-185. https://doi.org/10.4271/2015 -01 -1529

[14] Taherkhani, A. R. (2015). *Computational fluid dynamics based optimisation of emergency response vehicles*. University of Leeds.

[15] Roy, S. & Srinivasan, P. (2000). *External Flow Analysis of a Truck for Drag Reduction*. https://doi.org/10.4271/2000 -01 -3500

[16] Ferziger, J. H. & Peric, M. (2002). *Computational methods for fluid dynamics. 3. Rev*. https://doi.org/10.1007/978-3-642-56026-2

[17] Pham, H. (2006). *Springer handbook of engineering statistics*. Springer Science & Business Media. https://doi.org/10.1007/978-1-84628-288-1

[18] Oehlert, G. W. (2010). *A first course in design and analysis of experiments*.

[19] Rao, S. S. (2019). *Engineering optimization: Theory and practice*. John Wiley & Sons. https://doi.org/10.1002/9781119454816

Contact information:

Stjepan GALAMBOŠ, Assistant Professor
Faculty of Technical Sciences,
Trg Dositeja Obradovića 6, 21000 Novi Sad, Serbia
E-mail: galambos@uns.ac.rs

Nenad POZNANOVIĆ, Assistant Professor
(Corresponding author)
Faculty of Technical Sciences,
Trg Dositeja Obradovića 6, 21000 Novi Sad, Serbia
E-mail: npoz@uns.ac.rs

Nebojša NIKOLIĆ, Associate Professor
Faculty of Technical Sciences,
Trg Dositeja Obradovića 6, 21000 Novi Sad, Serbia
E-mail: nebnik@uns.ac.rs

Dragan RUŽIĆ, Associate Professor
Faculty of Technical Sciences,
Trg Dositeja Obradovića 6, 21000 Novi Sad, Serbia
E-mail: ruzic@uns.ac.rs

Jovan DORIĆ, Associate Professor
Faculty of Technical Sciences,
Trg Dositeja Obradovića 6, 21000 Novi Sad, Serbia
E-mail: j_doric@uns.ac.rs